



LHCb Note 2004-002
TRIG

PERFORMANCE OF LEVEL-0
WITH A
DI-ELECTRON TRIGGER
AND ALTERNATIVE SOLUTIONS

E. Rodrigues

eduardo.rodrigues@cern.ch

CERN

March 2004

Abstract

The inclusion in the Level-0 Trigger of a di-electron trigger is studied from a performance point of view. A simple implementation is proposed, investigated, and compared to other alternatives of electron triggers.

Contents

1	Introduction	3
2	Simulation and Data Samples	3
3	L0 Electron Candidates	5
3.1	Origin of L0 Electron Candidates	5
4	L0 Decision Unit Algorithms	8
4.1	TDR L0DU	8
4.2	Scenario 1 - Di-electron Trigger	9
4.3	Scenario 2 - Overriding Electron-trigger	9
4.4	Scenario 3 - Electron Trigger with 2 thresholds	9
4.5	Scenario 4 - Electron and Real Di-electron Triggers with 2 thresholds	9
5	Bandwidth Division Optimization	10
5.1	Thresholds	11
5.2	Sub-trigger Rates	13
6	Electron Trigger(s) Performance	14
6.1	Scenario 1 - Di-electron Trigger	14
6.2	Scenario 2 - Overriding Electron-trigger	22
6.3	Scenario 3 - Electron Trigger with 2 thresholds	22
6.4	Scenario 4 - Electron and Real Di-electron Triggers with 2 thresholds	24
7	L0 Performance Results	24
7.1	Scenario 1 - Di-electron Trigger	25
7.2	Scenario 2 - Overriding Electron-trigger	25
7.3	Scenario 3 - Electron Trigger with 2 thresholds	25
7.4	Scenario 4 - Electron and Real Di-electron Triggers with 2 thresholds	26
8	Implications for L1 and the HLT	36
9	Conclusions and Final Remarks	36

1 Introduction

At present, the Level-0 (L0) Decision Unit (L0DU) comprises a di-muon trigger, a special component as it is the only sub-trigger that can override the global event cuts (veto flag and multiplicity cuts). Its main purpose is to effectively detect di-muon events originating from the subsequent decay b-hadron $\rightarrow J/\psi + X \rightarrow (\mu^+\mu^-) + X$.

Though the usefulness of a similar di-electron trigger for b-hadron $\rightarrow J/\psi + X \rightarrow (e^+e^-) + X$ decays has been speculated for long, no detailed study had been made to assess the real pros and cons of the introduction of such a component in the L0DU.

At Level-1 (L1) di-muons are searched for, in order to reconstruct the $J/\psi \rightarrow \mu^+\mu^-$; but no $J/\psi \rightarrow e^+e^-$ mass reconstruction is yet available.

Recently, the usefulness of di-electrons at L1 was investigated in some detail [1]. It was concluded that a di-electron mass reconstruction at L1 can improve the efficiency for b-hadron $\rightarrow J/\psi + X \rightarrow (e^+e^-) + X$ decays by 10% of its present value provided an allocation of 10% of the L1-bandwidth to this "L1 sub-trigger" is affordable.

These conclusions were drawn based on the input information to L1 as given by the present L0DU settings summarized in the Trigger System Technical Design Report (TDR) [2]. Hence improvements might be expected with the inclusion of a dedicated di-electron trigger as early as in L0. This note investigates, from a performance point of view, the introduction of a di-electron trigger in the L0DU.

But the inclusion of a di-electron trigger at L0 is not straightforward; it would require changes in the hardware implementation, in order for the calorimeter trigger to also provide the second highest- E_T L0-electron candidate. Alternative solutions to the introduction of a di-electron trigger will be described and compared.

We first look at the nature and energy distributions of the L0-electron candidates. Section 4 details the four different scenarios of L0DU algorithms studied in this note. Next follow the studies of performance of the electron trigger in particular and of the whole L0 after the overall optimizations. We conclude with a comparison of the different approaches.

2 Simulation and Data Samples

All the simulation studies were done with samples of minimum-bias and B-decay signal events produced for the Trigger System TDR [2]. The offline selected signal events correspond to the selections described in [3]. Throughout the note we have used the following decay channels:

$$B_d^0 \rightarrow J/\psi(e^+e^-)K_S^0(\pi^+\pi^-) \text{ [4],}$$

$$B_d^0 \rightarrow K^{*0}(K^+\pi^-)\gamma \text{ [5],}$$

$$B_d^0 \rightarrow J/\psi(\mu^+\mu^-)K_S^0(\pi^+\pi^-) \text{ [6],}$$

$$\begin{aligned}
B_s^0 &\rightarrow J/\psi(\mu^+\mu^-, e^+e^-)\phi(K^+K^-) [7], \\
B_d^0 &\rightarrow \pi^+\pi^- [8], \\
B_s^0 &\rightarrow D_s^-(K^+K^-\pi^-)K^+ [9] \text{ and} \\
B_d^0 &\rightarrow \pi^+\pi^- + \pi^0 [10].
\end{aligned}$$

The data were generated with Brunel v17r4, SICBMC v260r2 and database v254r1.

We ran the L0 code at the nominal output rate of 1.0 MHz, corresponding to a minimum-bias retention of 6.74%.

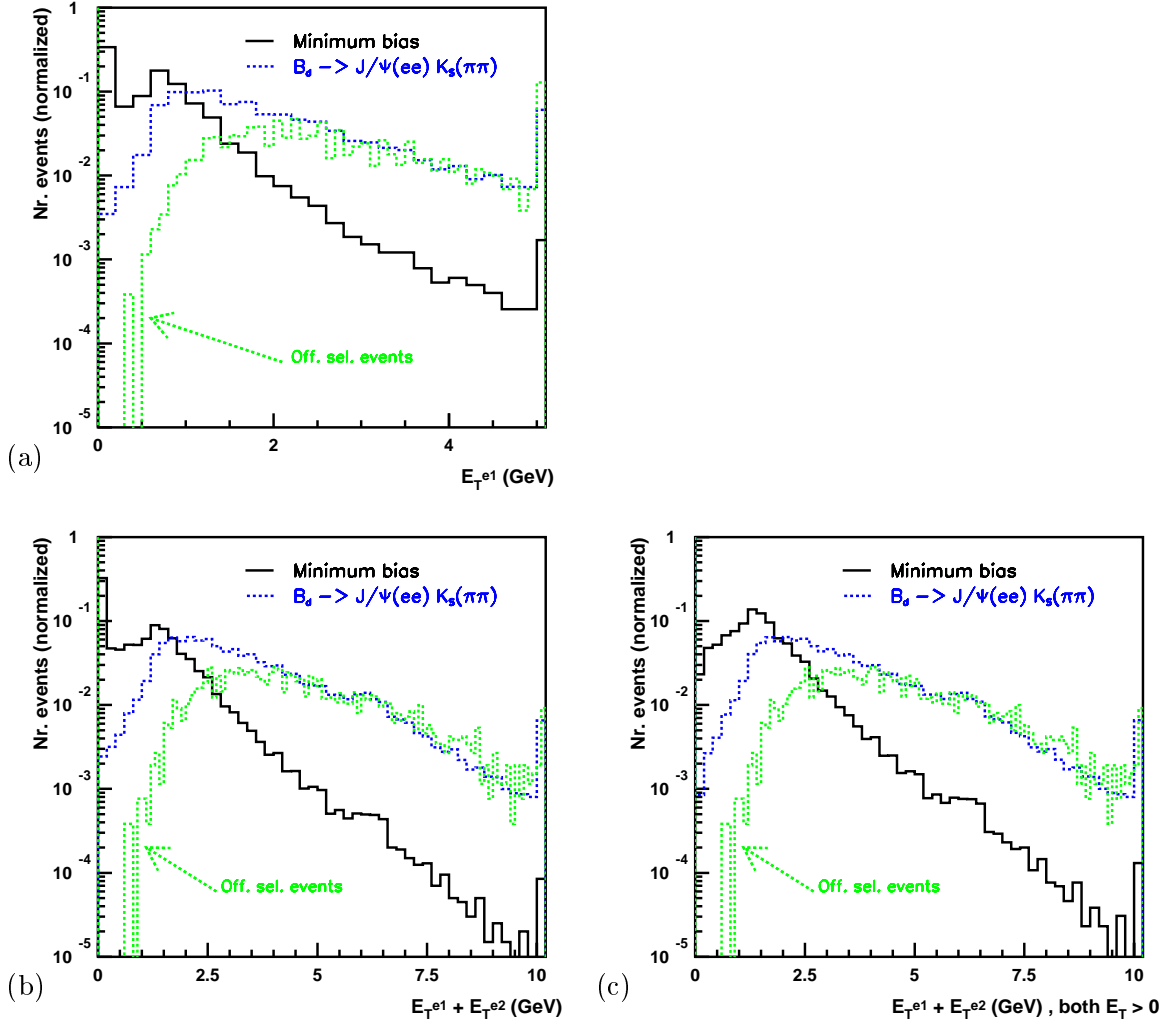


Figure 1: Transverse energy E_T distributions for (a) the highest- E_T L0-electron candidate (E_T^{e1}), for (b) the sum of the highest- and second highest- E_T L0-electron candidates ($E_T^{e1} + E_T^{e2}$), and (c) as in (b) but imposing that both $E_T^{e1}, E_T^{e2} > 0$. The various histograms correspond to minimum-bias events and to all and offline selected $B_d^0 \rightarrow J/\psi(e^+e^-)K_S^0(\pi^+\pi^-)$ events.

3 L0 Electron Candidates

In this section we take a closer look at the L0-electron candidates; we ordered them by decreasing transverse energy E_T . All signal events are offline selected $B_d^0 \rightarrow J/\psi(e^+e^-)K_S^0(\pi^+\pi^-)$ events, unless stated explicitly otherwise.

The transverse energy E_T distributions in minimum-bias and offline selected signal events for the highest- E_T and for the sum of the highest- and second highest- E_T L0-electron candidates are plotted in figure 1. The distributions are seen to have a different behaviour as a function of E_T : applying an electron cut above 2 GeV selects a large fraction of the signal events while rejecting the bulk of the minimum-bias. The effect is more pronounced for offline selected events, as expected. The same applies to the "di-electron" distribution (figures 1 (b)-(c)) but for a somewhat larger threshold. By di-electron distribution we mean the distribution of $E_T^{e1} + E_T^{e2}$. Figure 1 (c) is identical to (b) except that in the former case we impose that $E_T^{e1}, E_T^{e2} > 0$ where as this is not imposed in the latter case.

In trying to make use of the information contained in the second highest- E_T electron, possible correlations with the highest- E_T electron may be important and exploitable. Correlation plots will be shown in section 6 – devoted to the performance of the electron trigger(s) – after the different LODU algorithms have been presented and the optimizations performed.

3.1 Origin of L0 Electron Candidates

As stated in [1], if an electron from a J/ψ -decay emits a bremsstrahlung photon just before reaching the electromagnetic calorimeter (ECAL), and if the photon gets a large fraction of the electron's energy, then the Monte Carlo (MC) particle associated with the ECAL cluster will be the photon; and the J/ψ will be the grandmother of the photon. The L0 trigger will still consider the deposited energy in the ECAL to come from an electron due to the SPD hit.

Origin of highest- E_T L0-electrons				
all	100%			
& from signal-B	52%	100%		
& from J/ψ		98%	100%	$\approx 78\%/22\%$ are e^\pm/γ
& directly from J/ψ			70%	

Table 1: Origin of highest- E_T L0-electrons in $B_d^0 \rightarrow J/\psi(e^+e^-)K_S^0(\pi^+\pi^-)$ events: fraction of cases where they come from the signal-B decay, from the signal-B and (directly) from the $J/\psi \rightarrow e^+e^-$ decay.

Origin of 2 nd highest- E_T L0-electrons				
all	100%			
& from signal-B	28%	100%		
& from J/ ψ		96%	100%	$\approx 77\%/23\%$ are e^\pm/γ
& directly from J/ ψ			63%	

Table 2: Origin of 2nd highest- E_T L0-electrons in $B_d^0 \rightarrow J/\psi(e^+e^-)K_S^0(\pi^+\pi^-)$ events: fraction of cases where they come from the signal-B decay, from the signal-B and (directly) from the $J/\psi \rightarrow e^+e^-$ decay.

Origin of 3 rd highest- E_T L0-electrons				
all	100%			
& from signal-B	16%	100%		
& from J/ ψ		93%	100%	$\approx 76\%/24\%$ are e^\pm/γ
& directly from J/ ψ			53%	

Table 3: Origin of 3rd highest- E_T L0-electrons in $B_d^0 \rightarrow J/\psi(e^+e^-)K_S^0(\pi^+\pi^-)$ events: fraction of cases where they come from the signal-B decay, from the signal-B and (directly) from the $J/\psi \rightarrow e^+e^-$ decay.

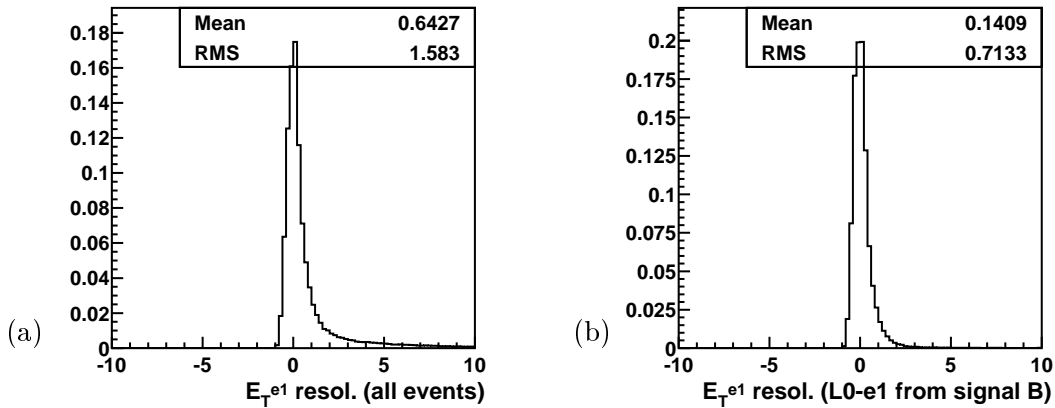


Figure 2: Transverse energy E_T^{e1} resolution of the highest- E_T L0-electron candidate in $B_d^0 \rightarrow J/\psi(e^+e^-)K_S^0(\pi^+\pi^-)$ signal decays for (a) all events and (b) for those events where the electron originates from the signal- J/ψ .

Probability (%)	all	L0-pass	selected	L0-pass & selected
1st electron	52	62	86	89
2nd electron	28	34	60	60
3rd electron	16	17	27	27
1st & 2nd electrons	19	25	52	53
1st & 3rd electrons	10	11	21	22

Table 4: Probabilities for the highest (1st), second highest (2nd) and third highest (3rd) E_T L0-electron candidates to come from the signal-B of $B_d^0 \rightarrow J/\psi(e^+e^-)K_S^0(\pi^+\pi^-)$ decays for all, L0-pass, offline selected and L0-pass and offline selected events. Note that the TDR L0DU was used to produce these numbers.

It is instructive to relate the L0-electron candidates to the MC truth information: a "higher depth" in the decay chain of the J/ψ is possible in case of (cascade) bremsstrahlung emission and/or subsequent γ conversion. In finding the origin of a L0-electron we followed up the complete decay chain to be sure not to miss such cases.

Tables 1-3 give an overview of the origin of the highest-, 2nd highest- and 3rd highest- E_T L0-electrons in signal events, respectively. For the highest- E_T electrons, about half of them come from the signal-B and are a daughter of the J/ψ ; but a third of these undergo bremsstrahlung (do not come directly from the J/ψ). And some 80% of the L0-electrons coming from the J/ψ decay are indeed electrons, fact that strengthens the good performance of the L0 calorimeter trigger. Similar conclusions can be drawn for the 2nd highest- and 3rd highest- E_T L0-electrons, though the contamination from the non-signal-B is more pronounced here. As expected, a larger fraction of these electrons has undergone bremsstrahlung, thereby losing energy.

The E_T resolution of the highest- E_T L0-electrons in signal events is plotted in figure 2. When the electron candidate comes from the signal-B the long tail becomes less important as a result of the different phase space considered.

In this note we are mainly concerned with the triggering at L0 of $J/\psi \rightarrow e^+e^-$ decays. We've looked at the origin of the L0-electrons independently, but how useful it is to use the combined information potentially present in the several candidates, not just the highest- E_T candidate? And how is the B-origin of these events affected by L0 and for offline selected events?

Table 4 collects all the information in the case of the L0 with the TDR settings: the second column shows how often the candidates come from the signal-B (as in tables 1-3), but it also shows it for the combination of the two highest- E_T electrons. For offline selected events these numbers are higher, as expected. It is remarkable that in about 90% of the offline selected events that pass L0 the highest- E_T L0-electron comes from the signal-B

decay. And in about half of the events both the two highest- E_T L0-electron candidates come from the signal-B.

It is based on these facts discussed in this section that one can hope to be able to improve the L0 efficiency using a di-electron trigger or a trigger that tries to profit from the B-origin of the electron candidates available to the L0DU.

4 L0 Decision Unit Algorithms

The L0DU detailed in the Trigger System TDR comprises the following components:

- total E_T ($\sum E_T$) cut;
- global event cuts: the Veto System decision and the hit multiplicities of the Veto System and the Scintillator Pad Detector (SPD);
- E_T thresholds on the sub-trigger components.

4.1 TDR L0DU

At present [2] the L0DU algorithm – TDR L0DU – issues a trigger decision based on the global event variables and on the transverse energies (or transverse momenta) reconstructed by the hadron, electron, photon, muon, di-muon and π^0 local and global triggers. Note that the di-muon trigger sums the transverse momenta of the two highest p_T muons – $\sum p_T^\mu$ – without the requirement that both their values are greater than zero, i. e. it is equivalent to the muon trigger if only one muon was found in the event.

The L0DU algorithm as described in the Trigger System TDR operates in the following way: an event triggers L0 if

- and only if the $\sum E_T$ is above 5.0 GeV, and
- it passes the global event selection and at least one of the L0 candidates passes its E_T threshold, or
- $\sum p_T^\mu$ (di-muon trigger) is above its threshold, irrespective of the global event cuts (only the $\sum E_T$ cut is applied).

The next sections will study the performance of L0 with a modified electron trigger and or extensions to it. Several scenarios will be analysed and compared; their definitions follow.

4.2 Scenario 1 - Di-electron Trigger

One can add to the L0DU a di-electron trigger just similar to the existing di-muon trigger. The L0DU algorithm then has an extra "component": an event can also trigger L0

- if and only if the $\sum E_T$ is above 5.0 GeV, and
- if $\sum E_T^e$ (di-electron trigger) is above its threshold, irrespective of the global event cuts.

As with the di-muon trigger, here $\sum E_T^e = E_T^{e1} + E_T^{e2}$, where E_T^{e1} (E_T^{e2}) is the transverse energy E_T of the (second) highest- E_T L0-electron candidate; and there is the possibility that $E_T^{e2} = 0$.

4.3 Scenario 2 - Overriding Electron-trigger

The electron component of the L0DU can also be modified such that it can override the global event cuts without the need for a di-electron trigger. In this second scenario all is as for the TDR except that for the electron trigger one has: an event also triggers L0

- if E_T^e (electron trigger) is above its threshold, irrespective of the global event cuts (only the $\sum E_T$ cut is applied).

4.4 Scenario 3 - Electron Trigger with 2 thresholds

One could also imagine an algorithm that would instead have 2 different thresholds for the electron trigger: a lower threshold for all events (just as the present electron trigger in the TDR L0DU), and a higher threshold able to override the global event cuts.

4.5 Scenario 4 - Electron and Real Di-electron Triggers with 2 thresholds

Ultimately one can consider an algorithm that comprises all of the "features" defining the previous scenarios: both an electron and a di-electron trigger with 2 thresholds. With such flexibility it is desirable to use the 2 sets of thresholds for 2 different types of events, classified by the result of the global event cuts.

And the di-electron trigger is defined as a real di-electron trigger: $\sum E_T^e = E_T^{e1} + E_T^{e2}$, where E_T^{e1} and $E_T^{e2} > 0$.

We propose the following algorithm done in sequence:

- an event only passes L0 if and only if the $\sum E_T$ is above 5.0 GeV

-
- For the hadron, muon and π^0 triggers the algorithm is as in the TDR:
 - an event passes L0 if it passes the global event selection and at least one of the L0 candidates passes its E_T threshold, or
 - if the Σp_T^μ (di-muon trigger) is above its threshold, irrespective of the global event cuts (only the ΣE_T cut is applied).
 - For the electron and di-electron triggers:
 - for those events that passed the global event cuts: the event passes L0 if the electron E_T^e or di-electron ΣE_T^e are above their respective thresholds;
 - for those events that did not pass the global event cuts: the event passes L0 if the electron or di-electron E_T are above their respective thresholds.

These two samples are therefore exclusive, with different dedicated thresholds.

5 Bandwidth Division Optimization

The optimization of the L0 bandwidth division consists in finding the sharing of the rates allocated to the various sub-triggers in such a way as to maximize the L0 performance. All details concerning this procedure have been described in a previous note [11]. We here merely remind the main points for completeness, and detail specific settings.

We've chosen here to characterize L0 by means of the following channels:

$$B_d^0 \rightarrow J/\psi(e^+e^-)K_S^0(\pi^+\pi^-),$$

$$B_d^0 \rightarrow K^{*0}(K^+\pi^-)\gamma,$$

$$B_d^0 \rightarrow J/\psi(\mu^+\mu^-)K_S^0(\pi^+\pi^-),$$

$$B_s^0 \rightarrow J/\psi(\mu^+\mu^-)\phi(K^+K^-),$$

$$B_d^0 \rightarrow \pi^+\pi^- \text{ and}$$

$$B_s^0 \rightarrow D_s^-(K^+K^-\pi^-)K^+.$$

First, each of these channels was optimized independently, to find $\varepsilon_{L0-\max}^{channel}$, the maximum trigger efficiency obtainable at L0 for this channel by adjusting the thresholds to give it the whole bandwidth. Then we maximized the quantity $\sum_{channels} \frac{\varepsilon_{L0}^{channel}}{\varepsilon_{L0-\max}^{channel}}$, (the sum running over the above-mentioned channels), $\varepsilon_{L0}^{channel}$ being the trigger efficiency using a set of thresholds for all channels simultaneously, i.e. by sharing the bandwidth between all representative channels.

All global event cuts were fixed to the values collected in table 5 (as in [2]). By itself alone the ΣE_T cut reduces to L0 output rate to ≈ 8.3 MHz; the rate is further reduced to 7 MHz after all the other global event cuts. In other words the global event selection rejects about 53% of minimum-bias events.

Global Event Cuts	Value	M. B. rate (kHz)	
Tracks in 2^{nd} vertex	3	} 8295 \pm 16	} 6981 \pm 17
Pile-Up Multiplicity	112 hits		
SPD Multiplicity	280 hits		
$\sum E_T$	5.0 GeV		

Table 5: List of L0 cuts on the global event variables. The last two columns give the inclusive L0 output rate on minimum-bias events after the $\sum E_T$ cut and after all four global event cuts (the uncertainties are statistical).

Trigger	E_T thresholds (GeV)				
	TDR	Scen. 1	Scen. 2	Scen. 3	Scen. 4
hadron	3.60	3.80	3.90	3.90	4.10
electron	2.80	3.10	2.40	low/high: 2.2/2.5	non-veto/veto: 3.60/4.00
photon	2.60	3.00	3.40	2.80	2.80
π_{local}^0	4.50	4.80	4.80	4.30	3.70
π_{global}^0	4.00	4.80	3.20	3.80	3.60
muon	1.10	1.10	1.10	1.10	1.10
Σp_T^μ	1.30	1.30	1.30	1.30	1.30
ΣE_T^e	–	3.60	–	–	non-veto/veto: 3.40/3.40

Table 6: List of L0 thresholds as in the Trigger TDR and obtained after the combined optimizations with the LODUs of scenarios 1-4 (cf. paragraphs 4 and 5). In the case of scenario 4 the ΣE_T^e trigger also requires that $E_T^{e1,2} > 0$. Refer to paragraphs 4.4 and 4.5 for details on the meaning of "low/high" and "non-veto/veto".

Only the L0 E_T thresholds were then allowed to vary in the optimizations. Note that in the overall L0 optimization the thresholds on the muon triggers were kept fixed to the values as determined for the TDR. In this way one ensures that this study of the electron trigger does not affect the L0 performance of muon channels.

5.1 Thresholds

The lists of thresholds obtained after the combined L0 optimizations with the LODUs of the TDR and scenarios 1-4 (cf. paragraphs 4.2- 4.5) are given in table 6. In all cases the hadron threshold is increased compared to the TDR value – often the same happens with other sub-triggers – to allow the electron or di-electron trigger to contribute to the L0 bandwidth. Scenario 4 is somewhat special in the sense that the electron and real di-electron triggers behave differently depending on whether an event has passed or not the

Trigger	Inclusive M. B. rate (kHz)							
	TDR		Scen. 1		Scen. 2		Scen. 3	
hadron	705 ± 7		593 ± 7		553 ± 6		553 ± 6	
electron	103 ± 3	} 282 ± 5	76 ± 2	} 399 ± 5	263 ± 4	} 470 ± 6	low: 226 ± 4	} 456 ± 6
photon	126 ± 3		79 ± 2		56 ± 2		high: 225 ± 4	
π_{local}^0	110 ± 3		91 ± 3		91 ± 3		99 ± 3	
π_{global}^0	145 ± 3		75 ± 2		301 ± 5		129 ± 3	
ΣE_{T}^e	-		297 ± 5		-		171 ± 4	
muon	110 ± 3	} 161 ± 3	110 ± 3	} 161 ± 3	110 ± 3	} 161 ± 3	110 ± 3	} 161 ± 3
Σp_{T}^μ	145 ± 3		145 ± 3		145 ± 3		145 ± 3	

Table 7: List of L0 inclusive rates on minimum-bias events (M. B. rate) corresponding to the L0 thresholds in table 6, after the four global event cuts. All uncertainties are statistical.

Trigger	Inclusive M. B. rate (kHz)	
	Scen. 4	
hadron	460 ± 6	
electron (non-veto)	49 ± 2	} 554 ± 6
electron (veto)	19 ± 1	
photon	99 ± 3	
π_{local}^0	205 ± 4	
π_{global}^0	204 ± 4	
$\Sigma E_{\text{T}}^e, E_{\text{T}}^{e1,2} > 0$ (non-veto)	225 ± 4	
$\Sigma E_{\text{T}}^e, E_{\text{T}}^{e1,2} > 0$ (veto)	137 ± 3	
muon	110 ± 3	} 161 ± 3
Σp_{T}^μ	145 ± 3	

Table 8: List of L0 inclusive rates on minimum-bias events (M. B. rate) corresponding to the L0 thresholds of scenario 4 (cf. table 6, last column), after the four global event cuts. All uncertainties are statistical.

global event cuts. As both "non-veto" and "veto" samples are exclusive, the overriding thresholds do not have to be above the standard thresholds for non-vetoed events, as is the case with the di-muon trigger at present.

5.2 Sub-trigger Rates

With these four sets of thresholds the corresponding bandwidth division – on minimum-bias events – for the hadron, electromagnetic (electron, photon and π^0 's, di-electron) and muon (muon and di-muon) triggers is, after the global event selection, as collected in tables 7-8; these tables also give a discriminative contribution from each sub-trigger. All rates are inclusive apart from the 2 electron and real di-electron rates in table 8, which are both exclusive between "non-veto" and "veto" samples. Compared to the TDR settings, all first three scenarios investigated result in a "transfer" of $\approx 100\text{--}150$ kHz of hadron trigger bandwidth to the electromagnetic triggers. For the fourth scenario – the electron and real di-electron triggers with 2 thresholds – this effect is even more pronounced: the hadron trigger loses a small third of its bandwidth in favour of the electromagnetic triggers that become the most bandwidth-consuming component of L0.

The fact that the overall L0 optimization favours such a configuration where the hadron trigger is not as prominent as in the past, but still resulting in relatively small losses for the hadronic channels after the combined L0 optimization (more details are given in paragraph 7 and tables therein), may seem puzzling at first. A study of this is underway and will be presented elsewhere [12].

It is instructive to see how the L0 rate depends on the thresholds. In figure 3 the output rate on minimum-bias events is shown inclusively for each of the (TDR) sub-triggers. By inclusive is meant that each sub-trigger is considered separately and by itself, the rate then being given after the global event cuts. The contribution from the di-electron trigger is also shown for comparison. The hadron trigger is by far the most "bandwidth-consuming" sub-trigger – it fills the whole L0 bandwidth with a threshold set around 3.2 GeV. The di-electron trigger is also seen to potentially take a large fraction of the bandwidth, due to the fact that two L0-electrons with sufficient E_T are often reconstructed at L0. On the other hand none of the muon triggers fill the full L0 bandwidth, even with the threshold of $E_T > 0$. Figure 4 shows a similar plot with the "overriding electron trigger" defined in section 4.3.

The special case of the electron and real di-electron triggers of scenario 4 is displayed in figure 5. As expected, at a given threshold, the rates are higher for the di-electron compared to the electron triggers; and also the rates are higher for non-vetoed than for vetoed events.

Probability (%)	all	L0-pass	selected	L0-pass & selected
1st electron	52	66	86	90
2nd electron	28	38	60	64
3rd electron	16	17	27	27
1st & 2nd electrons	19	28	52	57
1st & 3rd electrons	10	12	21	23

Table 9: Probabilities for the highest (1st), second highest (2nd) and third highest (3rd) E_T L0-electron candidates to come from the signal-B of $B_d^0 \rightarrow J/\psi(e^+e^-)K_S^0(\pi^+\pi^-)$ decays for all, L0-pass, offline selected and L0-pass and offline selected events. Note that the di-electron L0DU (scenario 1) was used to produce these numbers.

6 Electron Trigger(s) Performance

6.1 Scenario 1 - Di-electron Trigger

The di-electron trigger tries to exploit the information contained in the second highest- E_T electron. Table 9 is to be compared with table 4. The former gives the same probabilities obtained with the di-electron trigger. As expected, after L0, the probability that the second highest- E_T electron comes from the signal-B is higher: in close to 60% of the offline selected events that pass this L0 both the two highest- E_T L0-electron candidates come from the

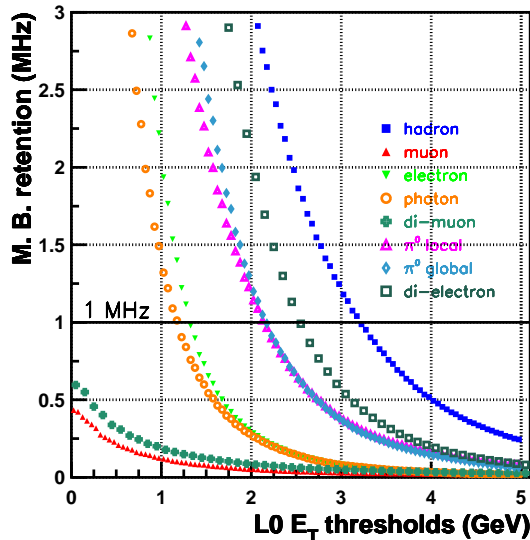


Figure 3: The L0 output rate for minimum-bias events (M. B. retention) as a function of the E_T cut for all "TDR sub-triggers". The di-electron trigger is included for comparison.

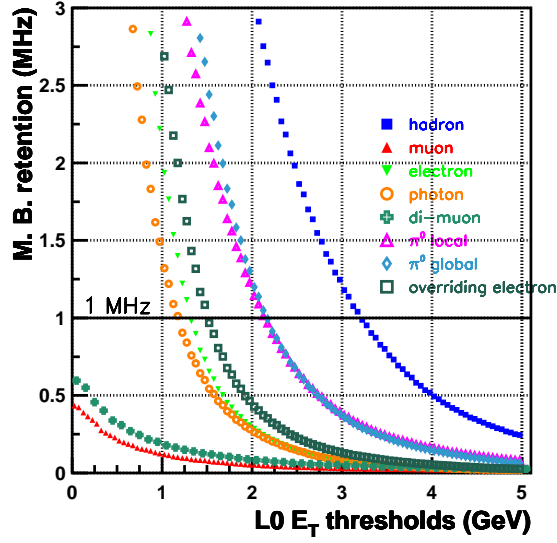


Figure 4: The L0 output rate for minimum-bias events (M. B. retention) as a function of the E_T cut for all "TDR sub-triggers". The overriding electron trigger is included for comparison.

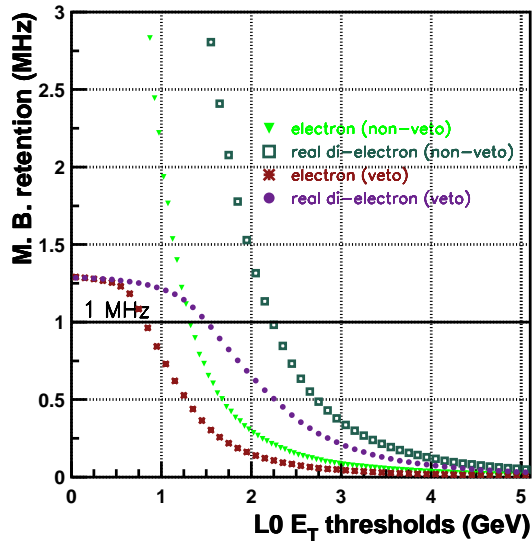


Figure 5: The L0 output rate for minimum-bias events (M. B. retention) as a function of the E_T electron and real di-electron cuts as defined with scenario 4: "non-veto" ("veto") curves refer to the curves obtained for events that pass (do not pass) the global event cuts; both sets are therefore exclusive.

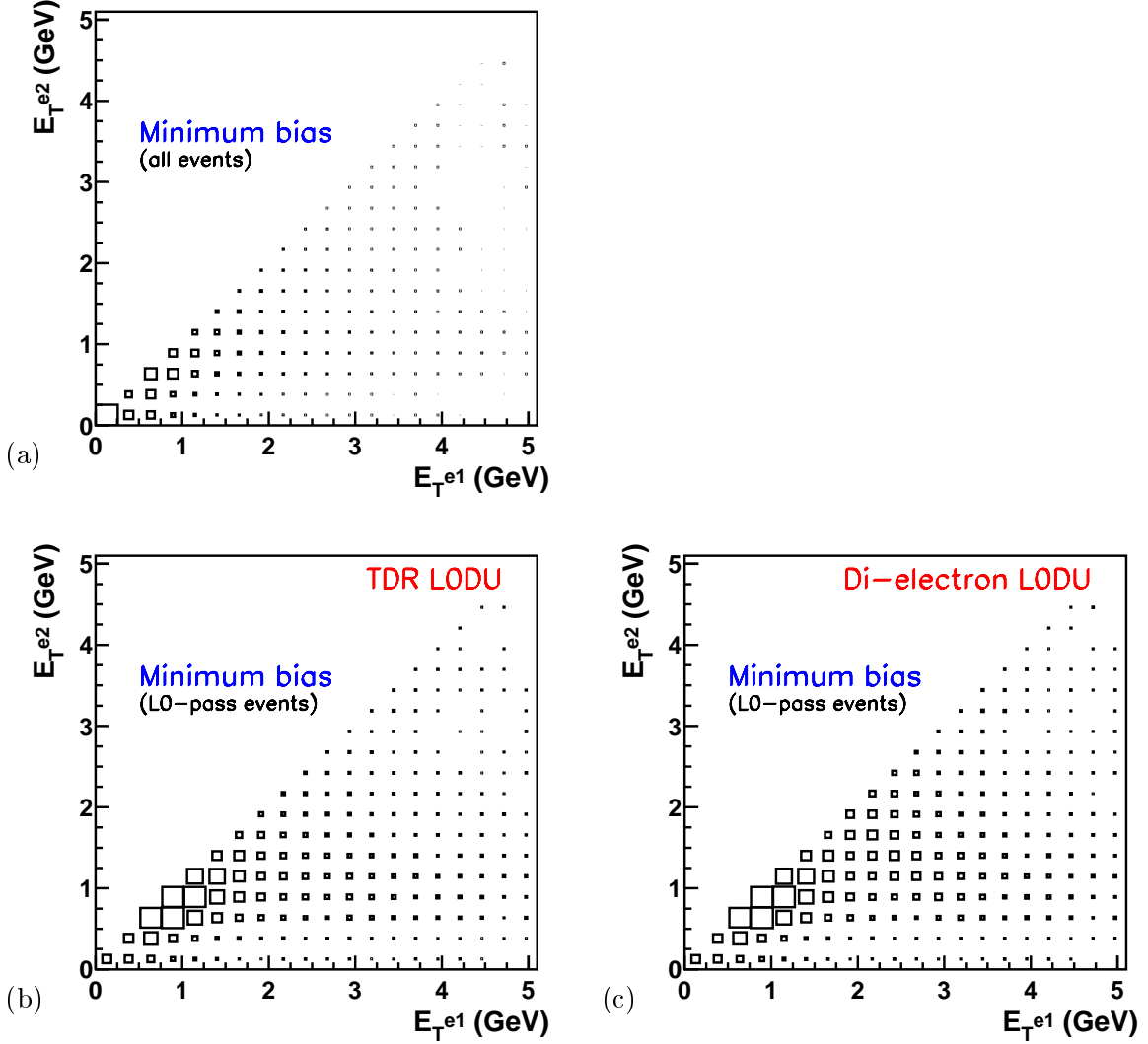


Figure 6: Correlation plots of the transverse energies of the highest- E_T (E_T^{e1}) and second highest- E_T (E_T^{e2}) L0-electron candidates in minimum-bias events. The scatter plots are for (a) all minimum-bias events, (b) for those events that pass the TDR L0DU, and for (c) those events that pass the L0DU with the di-electron trigger.

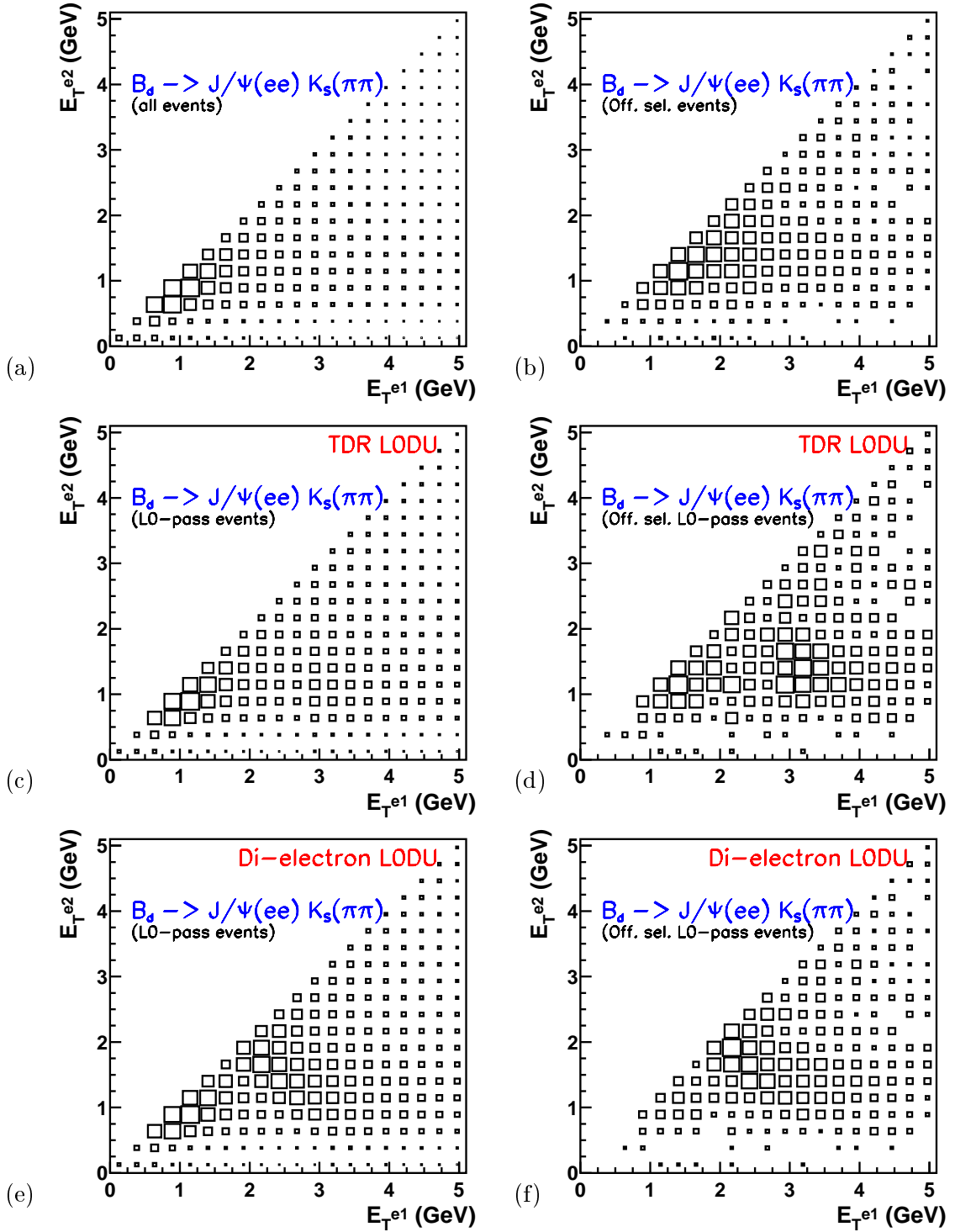


Figure 7: Correlation plots of the transverse energies of the highest- E_T (E_T^{e1}) and second highest- E_T (E_T^{e2}) L0-electron candidates in $B_d^0 \rightarrow J/\psi(e^+e^-)K_S^0(\pi^+\pi^-)$ events. The scatter plots are for (a) all events, (b) those passing the offline selection, (c) those that pass the TDR L0DU, (d) those that pass the TDR L0DU and the offline selection, (e) those that pass the L0DU with the di-electron trigger (scenario 1), and (f) those that pass the L0DU with the di-electron trigger and the offline selection.

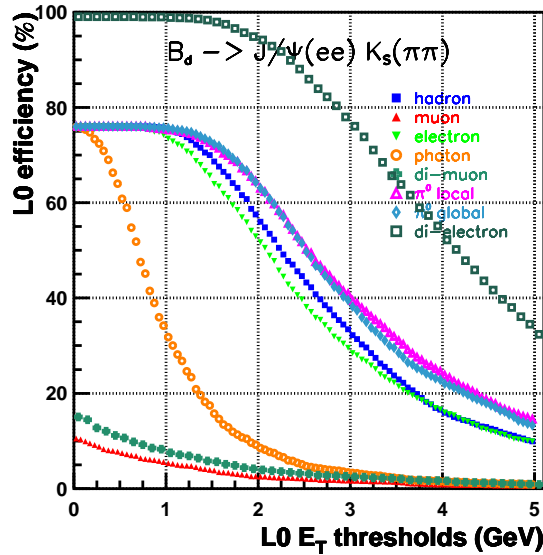


Figure 8: The L0 sub-triggers inclusive efficiencies as a function of the L0 thresholds for the $B_d^0 \rightarrow J/\psi(e^+e^-)K_S^0(\pi^+\pi^-)$ signal decay. Also the di-electron trigger is included for comparison (scenario 1).

signal-B.

Figures 6 and 7 show scatter plots of the E_T distributions of the two highest- E_T electrons for a multitude of situations, in minimum-bias and signal events, respectively. For minimum-bias events, both L0-electrons tend to have a higher E_T after L0, both with the TDR LODU and with the di-electron trigger (figure 6(b)-(c)). With the di-electron trigger some events get "picked up" with high E_T^{e1} and/or high-ish E_T^{e2} ; fact that does not occur with the TDR LODU (comparing (b) and (c) in figure 6). This fact tends to conclude that in the former case the di-electron sub-trigger is actually the responsible for some extra events passing L0, whereas in the latter case the L0-electrons correspond more to random triggering as far as the electron sub-trigger is concerned (e. g. electrons in events triggered by another sub-trigger).

The situation is different for signal events. Interesting is the effect of L0 on offline selected events (figure 7(b)). Comparing with figures 7(d),(f) it is striking how the E_T^{e2} versus E_T^{e1} distributions after L0 mimic better the distribution for selected events in the case of the di-electron trigger compared to the TDR L0.

Comparing both signal and minimum-bias events leads to a hint that the definition of a real di-electron trigger could be useful. Indeed no offline selected signal events are seen in the low E_T^{e2} region (figure 7(b)), whereas many such events are present in the minimum-bias sample (figure 6(a)) – for this particular B-signal channel the offline selection cuts at $E_T^{e2} > 0.5$ GeV, visible with some "noise" due to the L0 E_T resolution. This idea has been

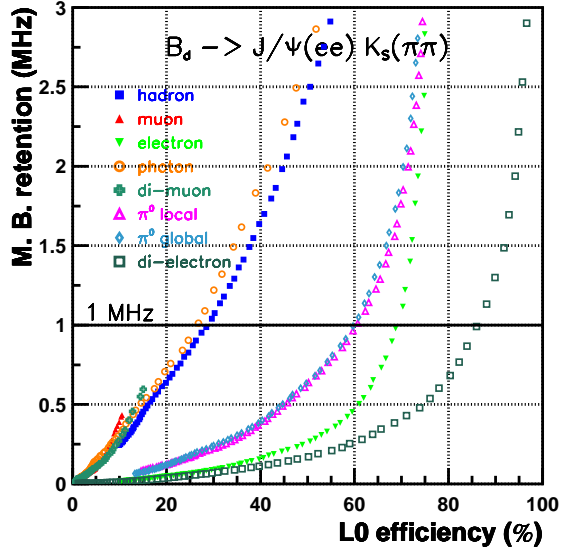


Figure 9: The L0 sub-triggers inclusive minimum-bias retentions as a function of the inclusive efficiencies for the $B_d^0 \rightarrow J/\psi(e^+e^-)K_S^0(\pi^+\pi^-)$ signal decay. Also the di-electron trigger is included for comparison (scenario 1).

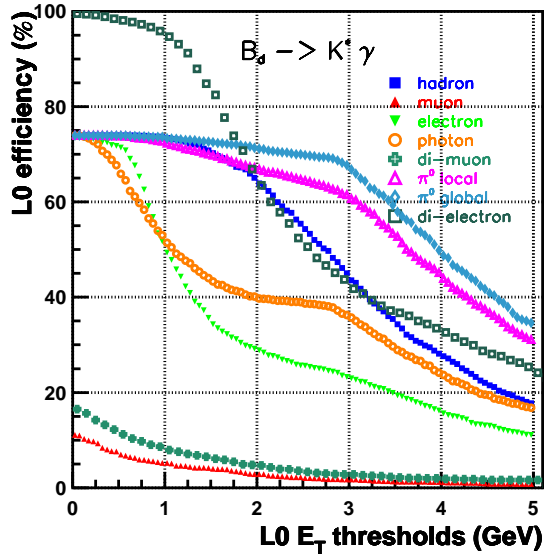


Figure 10: The L0 sub-triggers inclusive efficiencies as a function of the L0 thresholds for the $B_d^0 \rightarrow K^{*0}(K^+\pi^-)\gamma$ signal decay. Also the di-electron trigger is included for comparison (scenario 1).

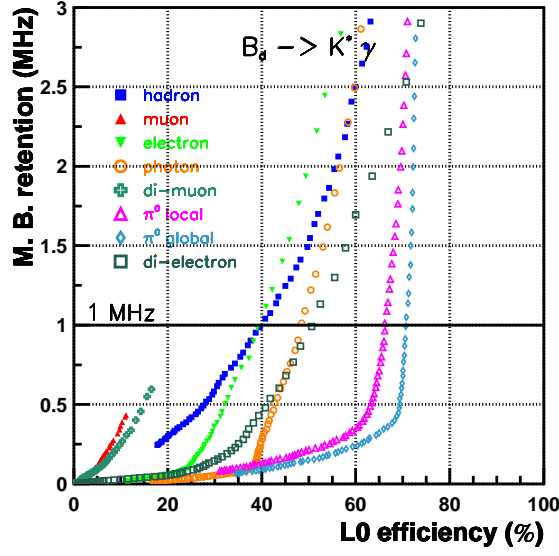


Figure 11: The L0 sub-triggers inclusive minimum-bias retentions as a function of the inclusive efficiencies for the $B_d^0 \rightarrow K^{*0}(K^+\pi^-)\gamma$ signal decay. Also the di-electron trigger is included for comparison (scenario 1).

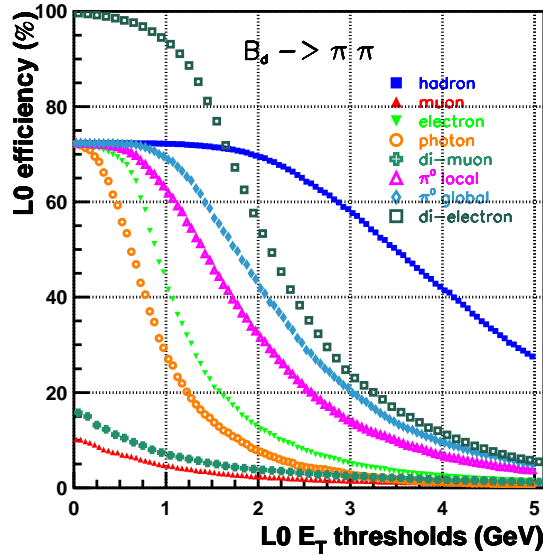


Figure 12: The L0 sub-triggers inclusive efficiencies as a function of the L0 thresholds for the $B_d^0 \rightarrow \pi^+\pi^-$ signal decay. Also the di-electron trigger is included for comparison (scenario 1).

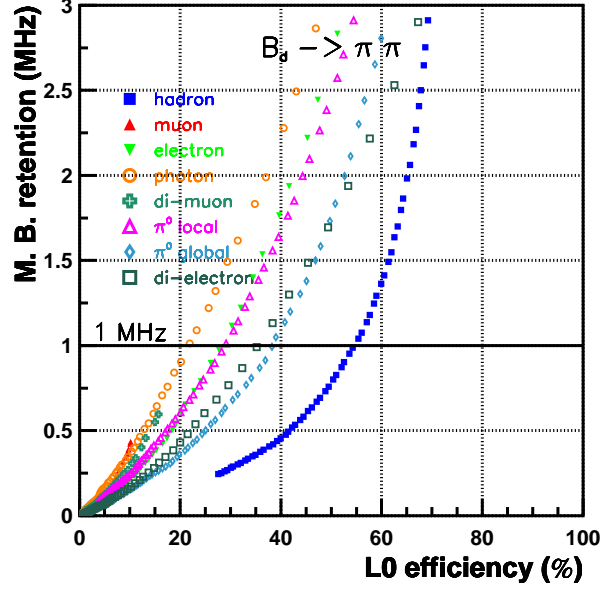


Figure 13: The L0 sub-triggers minimum-bias retentions as a function of the inclusive efficiencies for the $B_d^0 \rightarrow \pi^+\pi^-$ signal decay. Also the di-electron trigger is included for comparison (scenario 1).

exploited with the fourth scenario.

The performance of the electron and di-electron sub-triggers are compared with the performance of the other sub-triggers in figures 8 to 13, taking the examples of a "di-electron decay" ($B_d^0 \rightarrow J/\psi(e^+e^-)K_S^0(\pi^+\pi^-)$), a "photon decay" ($B_d^0 \rightarrow K^{*0}(K^+\pi^-)\gamma$) and a hadronic decay ($B_d^0 \rightarrow \pi^+\pi^-$). Also shown are the L0 efficiencies ε_{L0} as a function of the sub-trigger thresholds and the L0 minimum-bias retention rate as a function of ε_{L0} . Note, again, that each curve is inclusive, i. e., each sub-trigger is considered separately and by itself, the L0DU being the set of global event cuts and the sub-trigger.

For the $B_d^0 \rightarrow J/\psi(e^+e^-)K_S^0(\pi^+\pi^-)$ decay channel (figures 8-9), the di-electron sub-trigger is clearly the most performant – as expected given its definition – both at a given E_T threshold and for a given L0 minimum-bias output rate. It is still rather effective for the other channels since it can override the global event cuts and two electron candidates adding to a sufficient E_T are often found in an event (even if not coming from the signal-B).

Figures 8, 10 and 12 all have a common feature: one can distinguish three groups of sub-triggers with different behaviours. First, in all cases the muon triggers contribute very little to the L0 efficiency – this is opposite to what one would observe for a muon channel such as $B_d^0 \rightarrow J/\psi(\mu^+\mu^-)K_S^0(\pi^+\pi^-)$. Second, only the di-electron sub-trigger can reach an efficiency of 100% at very low threshold, thanks to the fact that it overrides the global event cuts. Third, all the other electromagnetic and the hadron sub-triggers are not able

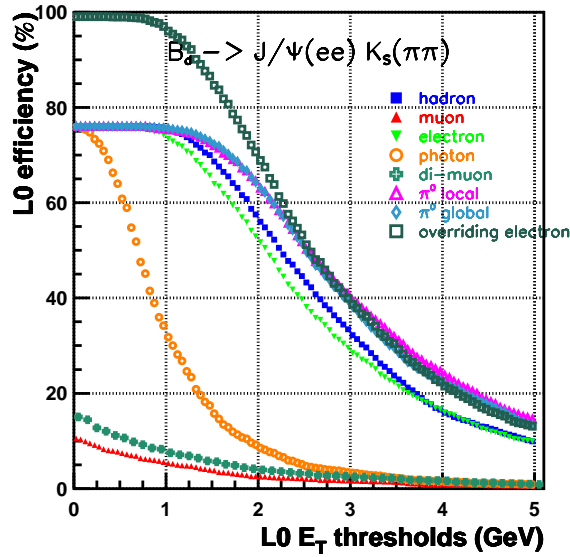


Figure 14: The L0 sub-triggers inclusive efficiencies as a function of the L0 thresholds for the $B_d^0 \rightarrow J/\psi(e^+e^-)K_S^0(\pi^+\pi^-)$ signal decay. Also the overriding electron trigger is included for comparison (scenario 2).

to go above a certain maximum efficiency even with the less restrictive $E_T > 0$ cut; this is the simple manifestation of the global event cuts, which remove alone $\approx 25\%$ of the signal events.

6.2 Scenario 2 - Overriding Electron-trigger

This overriding electron sub-trigger takes considerably less bandwidth than a di-electron sub-trigger. A corresponding difference in the E_T evolution of the L0 efficiency is observed (comparison between figures 14 and 8). Remarkably, the minimum-bias L0 output rate as a function of the L0 efficiency is rather similar for the di-electron trigger and the overriding electron trigger (comparison between figures 15 and 9). In other words, at constant inclusive L0 bandwidth, both sub-triggers have about the same performance for offline selected $B_d^0 \rightarrow J/\psi(e^+e^-)K_S^0(\pi^+\pi^-)$ events.

6.3 Scenario 3 - Electron Trigger with 2 thresholds

In this case the electron sub-trigger has a "standard" and an overriding component. Both have been discussed in the previous two paragraphs.

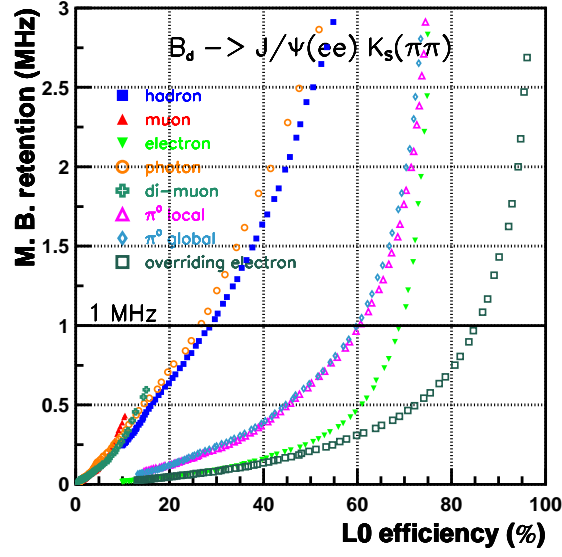


Figure 15: The L0 sub-triggers inclusive minimum-bias retentions as a function of the inclusive efficiencies for the $B_d^0 \rightarrow J/\psi(e^+e^-)K_S^0(\pi^+\pi^-)$ signal decay. Also the overriding electron trigger is included for comparison (scenario 2).

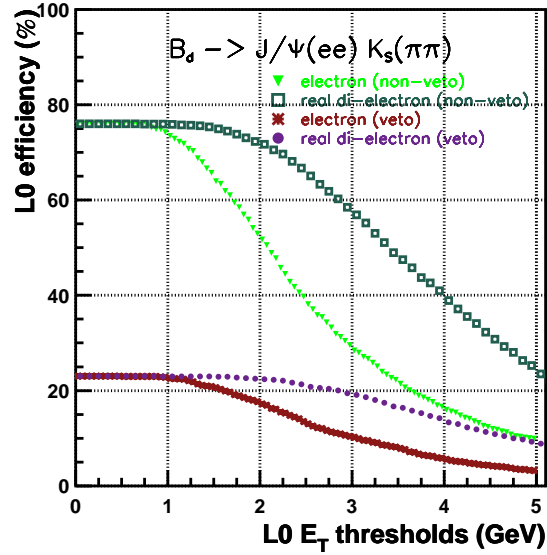


Figure 16: L0 sub-triggers inclusive efficiencies as a function of the L0 thresholds for the $B_d^0 \rightarrow J/\psi(e^+e^-)K_S^0(\pi^+\pi^-)$ signal decay. The "non-veto" ("veto") electron and real di-electron curves refer to the curves obtained with the L0DU scenario 4 for events that pass (do not pass) the global event cuts.

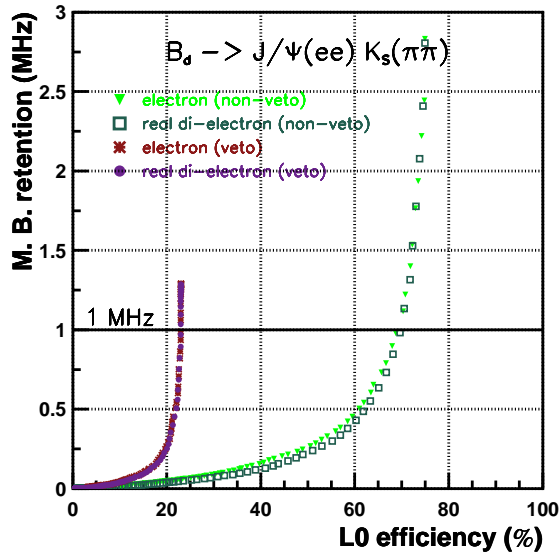


Figure 17: L0 sub-triggers inclusive minimum-bias retentions as a function of the inclusive efficiencies for the $B_d^0 \rightarrow J/\psi(e^+e^-)K_S^0(\pi^+\pi^-)$ signal decay. The "non-veto" ("veto") electron and real di-electron curves refer to the curves obtained with the L0DU scenario 4 for events that pass (do not pass) the global event cuts.

6.4 Scenario 4 - Electron and Real Di-electron Triggers with 2 thresholds

In this fourth scenario all but the electron and di-electron triggers are different from what has been described above. Figures 16-17 show, respectively, the L0 efficiencies ε_{L0} as a function of the sub-trigger thresholds and the L0 minimum-bias retention rate as a function of ε_{L0} . These curves require some care of interpretation: because the "non-veto" and "veto" samples are exclusive, the overall electron or di-electron efficiency is the combination of the respective efficiencies, which explains why one gets 100% summed efficiency at very low threshold. It is then clear that this scenario is most performant. The next paragraph will focus on a quantitative comparison of performances obtained with the different scenarios.

7 L0 Performance Results

In this section we detail the results obtained with the different L0DU scenarios after the overall optimizations of L0. In the following tables we will present the performance numbers for the set of B-signal decays used for the optimizations (listed in section 5) and the a posteriori performance numbers for two extra channels, chosen to be sensitive to the electromagnetic triggers and to cross-check the L0 performance; they are $B_s^0 \rightarrow J/\psi(e^+e^-)\phi(K^+K^-)$

and $B_d^0 \rightarrow \pi^+\pi^-\pi^0$.

The performance of L0 has been quantified by means of three sets of tables; we show results on $\varepsilon_{L0-\max}$ and ε_{L0} (defined in section 5), and on the inclusive efficiencies for the hadronic, electromagnetic and muon triggers.

7.1 Scenario 1 - Di-electron Trigger

With the inclusion of a di-electron trigger $\varepsilon_{L0-\max}$ is seen to improve substantially – compared to the TDR L0DU – for all the electromagnetic channels, including $B_d^0 \rightarrow K^{*0}(K^+\pi^-)\gamma$ (table 10); the improvement is of the order of 20% for b-hadron $\rightarrow J/\psi + X \rightarrow (e^+e^-) + X$ decays.

More important is the improvement in the efficiency ε_{L0} obtained with the overall L0 optimizations (table 11). Without affecting the hadronic and muon channels an improvement of the order of 45% is obtained for the b-hadron $\rightarrow J/\psi + X \rightarrow (e^+e^-) + X$ decays. Also the $B_d^0 \rightarrow K^{*0}(K^+\pi^-)\gamma$ channel improves by $\approx 10\%$ due to the correlations between the electron and photon triggers.

The corresponding inclusive efficiencies for the hadronic, electromagnetic and muon triggers are collected in table 12. For comparison the same efficiencies related to the TDR L0DU are shown in table 13. The increasing importance of the electromagnetic compared to that of the hadron trigger is clear.

Both $\varepsilon_{L0-\max}$ and ε_{L0} efficiencies for the hadronic and muon channels are basically unchanged with respect to the results presented in the Trigger TDR.

7.2 Scenario 2 - Overriding Electron-trigger

As seen from table 14, though not using any information from the second highest- E_T L0-electron, this electron trigger that overrides the global event cuts performs almost as well as the di-electron trigger for the b-hadron $\rightarrow J/\psi + X \rightarrow (e^+e^-) + X$ decays, the differences being of the order of 10%. And it is as performant in the case of $B_d^0 \rightarrow K^{*0}(K^+\pi^-)\gamma$.

The corresponding inclusive efficiencies for the hadronic, electromagnetic and muon triggers are in table 15.

Again, $\varepsilon_{L0-\max}$ and ε_{L0} for the hadronic and muon channels are almost unchanged with respect to the results presented in the Trigger TDR.

7.3 Scenario 3 - Electron Trigger with 2 thresholds

An electron trigger with two thresholds is as efficient as the overriding electron trigger (comparing table 16 to table 14). The inclusive efficiencies for the hadronic, electromagnetic

Decay Channel	$\varepsilon_{L0-max}(\%)$				
	TDR	Scen. 1	Scen. 2	Scen. 3	Scen. 4
$B_d^0 \rightarrow J/\psi(e^+e^-)K_S^0(\pi^+\pi^-)$	69.7 ± 0.9	85.0 ± 0.7	84.9 ± 0.7	84.8 ± 0.7	85.9 ± 0.7
$B_d^0 \rightarrow K^{*0}(K^+\pi^-)\gamma$	77.6 ± 1.0	86.8 ± 0.8	84.3 ± 0.9	84.5 ± 0.9	89.6 ± 0.8
$B_d^0 \rightarrow J/\psi(\mu^+\mu^-)K_S^0(\pi^+\pi^-)$	93.0 ± 0.4	93.2 ± 0.4	93.2 ± 0.4	93.2 ± 0.4	93.2 ± 0.4
$B_s^0 \rightarrow J/\psi(\mu^+\mu^-)\phi(K^+K^-)$	93.0 ± 0.1	93.0 ± 0.1	93.0 ± 0.1	93.0 ± 0.1	93.1 ± 0.1
$B_d^0 \rightarrow \pi^+\pi^-$	54.7 ± 0.4	56.7 ± 0.7	56.7 ± 0.7	56.7 ± 0.7	58.8 ± 0.6
$B_s^0 \rightarrow D_s^-(K^+K^-\pi^-)K^+$	48.2 ± 0.3	48.2 ± 0.4	48.2 ± 0.4	48.2 ± 0.4	48.4 ± 0.4
$B_s^0 \rightarrow J/\psi(e^+e^-)\phi(K^+K^-)$	67.3 ± 0.5	84.8 ± 0.6	84.8 ± 0.6	84.8 ± 0.6	85.2 ± 0.6
$B_d^0 \rightarrow \pi^+\pi^-\pi^0$	81.6 ± 1.5	86.2 ± 2.3	85.3 ± 2.4	85.3 ± 2.4	84.8 ± 2.4

Table 10: Maximum L0 efficiency after single channel optimization (ε_{L0-max}) for the TDR L0DU and the L0DU scenarios 1-4. All uncertainties are statistical.

and muon triggers are in table 17. Again, ε_{L0-max} and ε_{L0} for the hadron and muon channels are almost unchanged with respect to the results presented in the Trigger TDR.

7.4 Scenario 4 - Electron and Real Di-electron Triggers with 2 thresholds

This L0DU algorithm is seen to be the most performant of all from a global point of view. All in all both ε_{L0-max} (table 10) and ε_{L0} (table 18) are on average larger for all channels compared to the performances obtained with the other scenarios. In particular, a $\approx 50\%$ efficiency improvement – compared to the TDR L0DU – is obtained for b-hadron $\rightarrow J/\psi + X \rightarrow (e^+e^-) + X$ decays while still improving simultaneously on most of the other channels; only large multiplicity hadronic channels (here represented by $B_s^0 \rightarrow D_s^-(K^+K^-\pi^-)K^+$) seem to suffer slightly. Simultaneously the $B_d^0 \rightarrow K^{*0}(K^+\pi^-)\gamma$ channel improves by $\approx 15\%$.

The inclusive efficiencies for the hadronic, electromagnetic and muon triggers are in table 19.

To a large extent the success of such a L0DU algorithm is due on one hand to an electromagnetic trigger designed to be most sensitive to electromagnetic channels, in particular to di-electron decays through a dedicated sub-trigger; and on the other hand to the ability of the electromagnetic components of L0 to trigger rather efficiently even on hadronic channels [12]. This last point can easily be deduced from table 19 (and also from the corresponding tables for the other scenarios).

Decay Channel	$\varepsilon_{L0}(\%)$		Gain w.r.t TDR
	TDR	Scen. 1	
$B_d^0 \rightarrow J/\psi(e^+e^-)K_S^0(\pi^+\pi^-)$	48.3 ± 1.0	70.8 ± 0.9	+46.6
$B_d^0 \rightarrow K^{*0}(K^+\pi^-)\gamma$	72.9 ± 1.0	80.2 ± 1.0	+10.0
$B_d^0 \rightarrow J/\psi(\mu^+\mu^-)K_S^0(\pi^+\pi^-)$	89.3 ± 0.5	89.6 ± 0.5	+0.3
$B_s^0 \rightarrow J/\psi(\mu^+\mu^-)\phi(K^+K^-)$	89.7 ± 0.1	89.8 ± 0.1	+0.1
$B_d^0 \rightarrow \pi^+\pi^-$	53.6 ± 0.4	56.5 ± 0.7	+5.4
$B_s^0 \rightarrow D_s^-(K^+K^-\pi^-)K^+$	47.2 ± 0.3	47.4 ± 0.4	+0.4
$B_s^0 \rightarrow J/\psi(e^+e^-)\phi(K^+K^-)$	49.0 ± 0.6	72.0 ± 0.8	+46.9
$B_d^0 \rightarrow \pi^+\pi^-\pi^0$	77.2 ± 1.6	74.6 ± 2.9	-3.4

Table 11: L0 efficiency after combined optimization of the L0 trigger (ε_{L0}) for the TDR L0DU and the L0DU scenario 1; and gain in efficiency with respect to the TDR results ($(\varepsilon_{L0}^{\text{Scen.1}} - \varepsilon_{L0}^{\text{TDR}})/\varepsilon_{L0}^{\text{TDR}}$). All uncertainties are statistical.

Decay Channel	$\varepsilon_{L0}(\%)$	Scen. 1 - Inclusive efficiencies (%)		
		had. trig.	elec. trig.	muon trig.
$B_d^0 \rightarrow J/\psi(e^+e^-)K_S^0(\pi^+\pi^-)$	70.8 ± 0.9	18.5 ± 0.8	64.9 ± 0.9	7.0 ± 0.5
$B_d^0 \rightarrow K^{*0}(K^+\pi^-)\gamma$	80.2 ± 1.0	30.0 ± 1.1	75.2 ± 1.1	7.5 ± 0.7
$B_d^0 \rightarrow J/\psi(\mu^+\mu^-)K_S^0(\pi^+\pi^-)$	89.6 ± 0.5	16.1 ± 0.6	13.0 ± 0.6	87.0 ± 0.6
$B_s^0 \rightarrow J/\psi(\mu^+\mu^-)\phi(K^+K^-)$	89.8 ± 0.1	17.5 ± 0.2	12.7 ± 0.2	87.3 ± 0.2
$B_d^0 \rightarrow \pi^+\pi^-$	56.5 ± 0.7	44.7 ± 0.7	19.8 ± 0.5	6.4 ± 0.3
$B_s^0 \rightarrow D_s^-(K^+K^-\pi^-)K^+$	47.4 ± 0.4	35.3 ± 0.4	16.2 ± 0.3	8.5 ± 0.3
$B_s^0 \rightarrow J/\psi(e^+e^-)\phi(K^+K^-)$	72.0 ± 0.8	20.5 ± 0.7	65.8 ± 0.9	7.1 ± 0.5
$B_d^0 \rightarrow \pi^+\pi^-\pi^0$	74.6 ± 2.9	36.1 ± 3.2	66.4 ± 3.2	8.9 ± 1.9

Table 12: L0 inclusive efficiencies for the hadronic, electromagnetic (electron, photon, π^0 's) and muon triggers. These were obtained after the optimization of the L0 trigger using the L0DU scenario 1, with the resulting efficiencies being reshown (for easy reference) in the second column. All uncertainties are statistical.

Decay Channel	$\varepsilon_{L0}(\%)$	TDR - Inclusive efficiencies (%)		
		had. trig.	elec. trig.	muon trig.
$B_d^0 \rightarrow J/\psi(e^+e^-)K_S^0(\pi^+\pi^-)$	48.3 ± 1.0	21.5 ± 0.8	37.4 ± 0.9	7.0 ± 0.5
$B_d^0 \rightarrow K^{*0}(K^+\pi^-)\gamma$	72.9 ± 1.0	32.7 ± 1.1	68.1 ± 1.1	7.8 ± 0.6
$B_d^0 \rightarrow J/\psi(\mu^+\mu^-)K_S^0(\pi^+\pi^-)$	89.3 ± 0.5	18.6 ± 0.7	8.3 ± 0.5	87.2 ± 0.6
$B_s^0 \rightarrow J/\psi(\mu^+\mu^-)\phi(K^+K^-)$	89.7 ± 0.1	20.0 ± 0.2	8.4 ± 0.1	87.4 ± 0.1
$B_d^0 \rightarrow \pi^+\pi^-$	53.6 ± 0.4	47.6 ± 0.5	14.1 ± 0.3	6.8 ± 0.2
$B_s^0 \rightarrow D_s^-(K^+K^-\pi^-)K^+$	47.2 ± 0.3	39.4 ± 0.3	11.7 ± 0.2	8.2 ± 0.2
$B_s^0 \rightarrow J/\psi(e^+e^-)\phi(K^+K^-)$	49.0 ± 0.6	22.9 ± 0.5	38.3 ± 0.5	7.0 ± 0.3
$B_d^0 \rightarrow \pi^+\pi^-\pi^0$	77.2 ± 1.6	39.4 ± 1.9	66.2 ± 1.8	7.9 ± 1.1

Table 13: L0 inclusive efficiencies for the hadronic, electromagnetic (electron, photon, π^0 's) and muon triggers. These were obtained after the optimization of the L0 trigger using the TDR L0DU (table taken from [11]), with the resulting efficiencies being reshown (for easy reference) in the second column. All uncertainties are statistical.

Decay Channel	$\varepsilon_{L0}(\%)$		Gain w.r.t TDR
	TDR	Scen. 2	
$B_d^0 \rightarrow J/\psi(e^+e^-)K_S^0(\pi^+\pi^-)$	48.3 ± 1.0	66.3 ± 0.9	+37.3
$B_d^0 \rightarrow K^{*0}(K^+\pi^-)\gamma$	72.9 ± 1.0	81.8 ± 1.0	+12.2
$B_d^0 \rightarrow J/\psi(\mu^+\mu^-)K_S^0(\pi^+\pi^-)$	89.3 ± 0.5	89.6 ± 0.5	+0.3
$B_s^0 \rightarrow J/\psi(\mu^+\mu^-)\phi(K^+K^-)$	89.7 ± 0.1	89.8 ± 0.1	+0.1
$B_d^0 \rightarrow \pi^+\pi^-$	53.6 ± 0.4	56.3 ± 0.7	+5.0
$B_s^0 \rightarrow D_s^-(K^+K^-\pi^-)K^+$	47.2 ± 0.3	46.7 ± 0.4	-1.1
$B_s^0 \rightarrow J/\psi(e^+e^-)\phi(K^+K^-)$	49.0 ± 0.6	68.4 ± 0.8	+39.6
$B_d^0 \rightarrow \pi^+\pi^-\pi^0$	77.2 ± 1.6	78.6 ± 2.7	+1.8

Table 14: L0 efficiency after combined optimization of the L0 trigger (ε_{L0}) for the TDR L0DU and the L0DU scenario 2; and gain in efficiency with respect to the TDR results ($(\varepsilon_{L0}^{\text{Scen.2}} - \varepsilon_{L0}^{\text{TDR}})/\varepsilon_{L0}^{\text{TDR}}$). All uncertainties are statistical.

Decay Channel	$\varepsilon_{L0}(\%)$	Scen. 2 - Inclusive efficiencies (%)		
		had. trig.	elec. trig.	muon trig.
$B_d^0 \rightarrow J/\psi(e^+e^-)K_S^0(\pi^+\pi^-)$	66.3 ± 0.9	17.3 ± 0.7	60.7 ± 1.0	7.0 ± 0.5
$B_d^0 \rightarrow K^{*0}(K^+\pi^-)\gamma$	81.8 ± 1.0	29.2 ± 1.1	78.6 ± 1.0	7.5 ± 0.7
$B_d^0 \rightarrow J/\psi(\mu^+\mu^-)K_S^0(\pi^+\pi^-)$	89.6 ± 0.5	15.2 ± 0.6	14.6 ± 0.6	87.0 ± 0.6
$B_s^0 \rightarrow J/\psi(\mu^+\mu^-)\phi(K^+K^-)$	89.8 ± 0.1	16.7 ± 0.2	14.6 ± 0.2	87.2 ± 0.2
$B_d^0 \rightarrow \pi^+\pi^-$	56.3 ± 0.7	43.5 ± 0.7	25.5 ± 0.6	6.4 ± 0.3
$B_s^0 \rightarrow D_s^-(K^+K^-\pi^-)K^+$	46.7 ± 0.4	33.8 ± 0.4	19.4 ± 0.4	8.5 ± 0.3
$B_s^0 \rightarrow J/\psi(e^+e^-)\phi(K^+K^-)$	68.4 ± 0.8	19.5 ± 0.7	73.0 ± 3.0	8.9 ± 1.9
$B_d^0 \rightarrow \pi^+\pi^-\pi^0$	78.6 ± 2.7	35.6 ± 3.2	62.9 ± 0.9	7.1 ± 0.5

Table 15: L0 inclusive efficiencies for the hadronic, electromagnetic (electron, photon, π^0 's) and muon triggers. These were obtained after the optimization of the L0 trigger using the L0DU scenario 2, with the resulting efficiencies being reshown (for easy reference) in the second column. All uncertainties are statistical.

Decay Channel	$\varepsilon_{L0}(\%)$		Gain w.r.t TDR
	TDR	Scen. 3	
$B_d^0 \rightarrow J/\psi(e^+e^-)K_S^0(\pi^+\pi^-)$	48.3 ± 1.0	68.7 ± 0.9	+42.2
$B_d^0 \rightarrow K^{*0}(K^+\pi^-)\gamma$	72.9 ± 1.0	83.0 ± 0.9	+13.9
$B_d^0 \rightarrow J/\psi(\mu^+\mu^-)K_S^0(\pi^+\pi^-)$	89.3 ± 0.5	89.8 ± 0.5	+0.6
$B_s^0 \rightarrow J/\psi(\mu^+\mu^-)\phi(K^+K^-)$	89.7 ± 0.1	90.0 ± 0.1	+0.3
$B_d^0 \rightarrow \pi^+\pi^-$	53.6 ± 0.4	55.5 ± 0.7	+3.5
$B_s^0 \rightarrow D_s^-(K^+K^-\pi^-)K^+$	47.2 ± 0.3	46.3 ± 0.4	-1.9
$B_s^0 \rightarrow J/\psi(e^+e^-)\phi(K^+K^-)$	49.0 ± 0.6	70.4 ± 0.8	+43.7
$B_d^0 \rightarrow \pi^+\pi^-\pi^0$	77.2 ± 1.6	77.7 ± 2.8	+0.6

Table 16: L0 efficiency after combined optimization of the L0 trigger (ε_{L0}) for the TDR L0DU and the L0DU scenario 3; and gain in efficiency with respect to the TDR results ($(\varepsilon_{L0}^{\text{Scen.3}} - \varepsilon_{L0}^{\text{TDR}})/\varepsilon_{L0}^{\text{TDR}}$). All uncertainties are statistical.

Decay Channel	$\varepsilon_{L0}(\%)$	Scen. 3 - Inclusive efficiencies (%)		
		had. trig.	elec. trig.	muon trig.
$B_d^0 \rightarrow J/\psi(e^+e^-)K_S^0(\pi^+\pi^-)$	68.7 ± 0.9	17.3 ± 0.7	63.7 ± 0.9	7.0 ± 0.5
$B_d^0 \rightarrow K^{*0}(K^+\pi^-)\gamma$	83.0 ± 0.9	29.3 ± 1.1	80.1 ± 1.0	7.5 ± 0.7
$B_d^0 \rightarrow J/\psi(\mu^+\mu^-)K_S^0(\pi^+\pi^-)$	89.8 ± 0.5	15.2 ± 0.6	13.6 ± 0.6	87.2 ± 0.6
$B_s^0 \rightarrow J/\psi(\mu^+\mu^-)\phi(K^+K^-)$	90.0 ± 0.1	16.7 ± 0.2	13.8 ± 0.2	87.5 ± 0.2
$B_d^0 \rightarrow \pi^+\pi^-$	55.5 ± 0.7	43.6 ± 0.6	23.1 ± 0.6	6.4 ± 0.3
$B_s^0 \rightarrow D_s^-(K^+K^-\pi^-)K^+$	46.3 ± 0.4	33.9 ± 0.4	18.2 ± 0.3	8.5 ± 0.3
$B_s^0 \rightarrow J/\psi(e^+e^-)\phi(K^+K^-)$	70.4 ± 0.8	19.5 ± 0.7	65.2 ± 0.9	7.2 ± 0.5
$B_d^0 \rightarrow \pi^+\pi^-\pi^0$	77.7 ± 2.8	35.7 ± 3.2	71.9 ± 3.0	8.9 ± 1.9

Table 17: L0 inclusive efficiencies for the hadronic, electromagnetic (electron, photon, π^0 's) and muon triggers. These were obtained after the optimization of the L0 trigger using the L0DU scenario 3, with the resulting efficiencies being reshown (for easy reference) in the second column. All uncertainties are statistical.

Decay Channel	$\varepsilon_{L0}(\%)$		Gain w.r.t TDR
	TDR	Scen. 4	
$B_d^0 \rightarrow J/\psi(e^+e^-)K_S^0(\pi^+\pi^-)$	48.3 ± 1.0	74.7 ± 0.9	+54.7
$B_d^0 \rightarrow K^{*0}(K^+\pi^-)\gamma$	72.9 ± 1.0	83.9 ± 0.9	+15.1
$B_d^0 \rightarrow J/\psi(\mu^+\mu^-)K_S^0(\pi^+\pi^-)$	89.3 ± 0.5	89.7 ± 0.5	+0.5
$B_s^0 \rightarrow J/\psi(\mu^+\mu^-)\phi(K^+K^-)$	89.7 ± 0.1	90.0 ± 0.1	+0.3
$B_d^0 \rightarrow \pi^+\pi^-$	53.6 ± 0.3	55.7 ± 0.7	+3.9
$B_s^0 \rightarrow D_s^-(K^+K^-\pi^-)K^+$	47.2 ± 0.3	45.9 ± 0.4	-2.8
$B_s^0 \rightarrow J/\psi(e^+e^-)\phi(K^+K^-)$	49.0 ± 0.6	75.2 ± 0.8	+53.5
$B_d^0 \rightarrow \pi^+\pi^-\pi^0$	77.2 ± 1.6	79.5 ± 2.7	+3.0

Table 18: L0 efficiency after combined optimization of the L0 trigger (ε_{L0}) for the TDR L0DU and the L0DU scenario 4; and gain in efficiency with respect to the TDR results ($(\varepsilon_{L0}^{\text{Scen.4}} - \varepsilon_{L0}^{\text{TDR}})/\varepsilon_{L0}^{\text{TDR}}$). All uncertainties are statistical.

Decay Channel	$\varepsilon_{L0}(\%)$	Scen. 4 - Inclusive efficiencies (%)		
		had. trig.	elec. trig.	muon trig.
$B_d^0 \rightarrow J/\psi(e^+e^-)K_S^0(\pi^+\pi^-)$	74.7 ± 0.9	15.3 ± 0.7	71.1 ± 0.9	7.0 ± 0.5
$B_d^0 \rightarrow K^{*0}(K^+\pi^-)\gamma$	83.9 ± 0.9	26.6 ± 1.1	81.3 ± 1.0	7.5 ± 0.7
$B_d^0 \rightarrow J/\psi(\mu^+\mu^-)K_S^0(\pi^+\pi^-)$	89.7 ± 0.5	13.0 ± 0.6	16.6 ± 0.7	87.1 ± 0.6
$B_s^0 \rightarrow J/\psi(\mu^+\mu^-)\phi(K^+K^-)$	90.0 ± 0.1	14.4 ± 0.2	16.9 ± 0.2	87.4 ± 0.2
$B_d^0 \rightarrow \pi^+\pi^-$	55.7 ± 0.7	40.2 ± 0.6	27.0 ± 0.6	6.4 ± 0.3
$B_s^0 \rightarrow D_s^-(K^+K^-\pi^-)K^+$	45.9 ± 0.4	30.5 ± 0.4	21.6 ± 0.4	8.5 ± 0.3
$B_s^0 \rightarrow J/\psi(e^+e^-)\phi(K^+K^-)$	75.2 ± 0.8	16.9 ± 0.7	71.8 ± 0.8	7.2 ± 0.5
$B_d^0 \rightarrow \pi^+\pi^-\pi^0$	79.5 ± 2.7	33.5 ± 3.0	74.5 ± 2.9	8.9 ± 1.9

Table 19: L0 inclusive efficiencies for the hadronic, electromagnetic (electron, photon, π^0 's) and muon triggers. These were obtained after the optimization of the L0 trigger using the L0DU scenario 4, with the resulting efficiencies being reshown (for easy reference) in the second column. All uncertainties are statistical.

Decay Channel	% global-vetoed L0-pass events				
	TDR	Scen. 1	Scen. 2	Scen. 3	Scen. 4
$B_d^0 \rightarrow J/\psi(e^+e^-)K_S^0(\pi^+\pi^-)$	4	23	22	20	23
$B_d^0 \rightarrow K^{*0}(K^+\pi^-)\gamma$	4	15	14	14	15
$B_d^0 \rightarrow J/\psi(\mu^+\mu^-)K_S^0(\pi^+\pi^-)$	24	24	24	24	24
$B_s^0 \rightarrow J/\psi(\mu^+\mu^-)\phi(K^+K^-)$	26	26	26	26	26
$B_d^0 \rightarrow \pi^+\pi^-$	4	14	12	11	15
$B_s^0 \rightarrow D_s^-(K^+K^-\pi^-)K^+$	5	13	12	11	14
$B_s^0 \rightarrow J/\psi(e^+e^-)\phi(K^+K^-)$	4	25	24	23	25
$B_d^0 \rightarrow \pi^+\pi^-\pi^0$	1	7	6	6	7
Minimum bias	5	15	13	12	18

Table 20: Percentage of offline selected signal and minimum-bias events that pass L0 but had been vetoed by the global event cuts (i. e. the event was overridden by an appropriate sub-trigger).

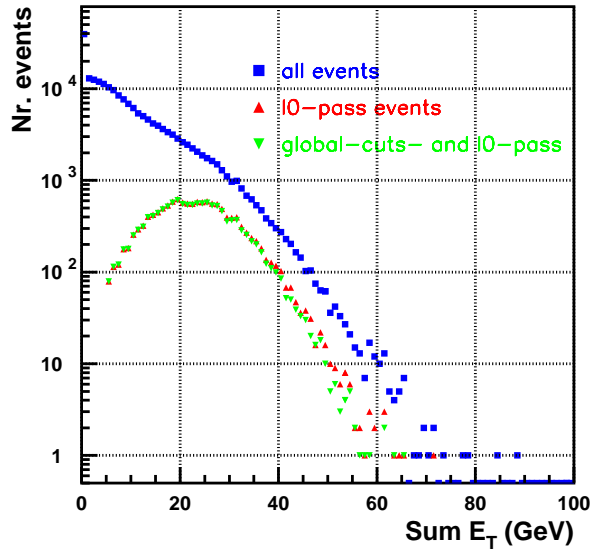


Figure 18: ΣE_T distributions for minimum-bias events and with the TDR L0DU.

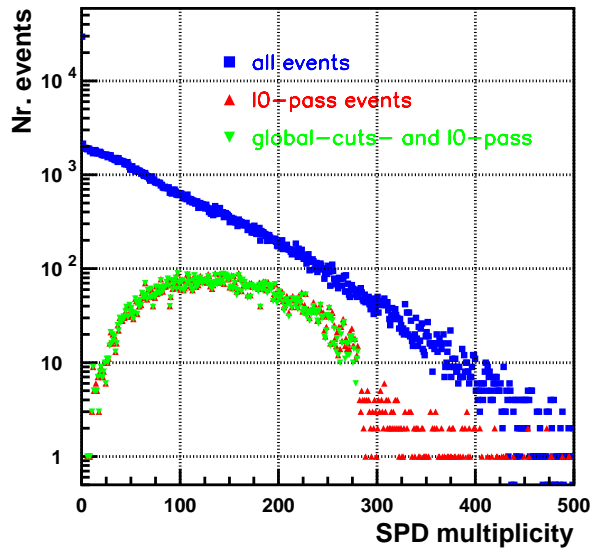


Figure 19: SPD multiplicity distributions for minimum-bias events and with the TDR L0DU.

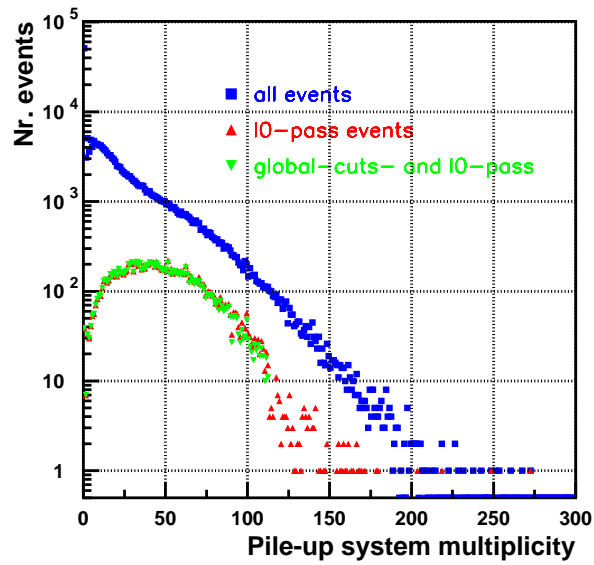


Figure 20: Pile-up system multiplicity distributions for minimum-bias events and with the TDR L0DU.

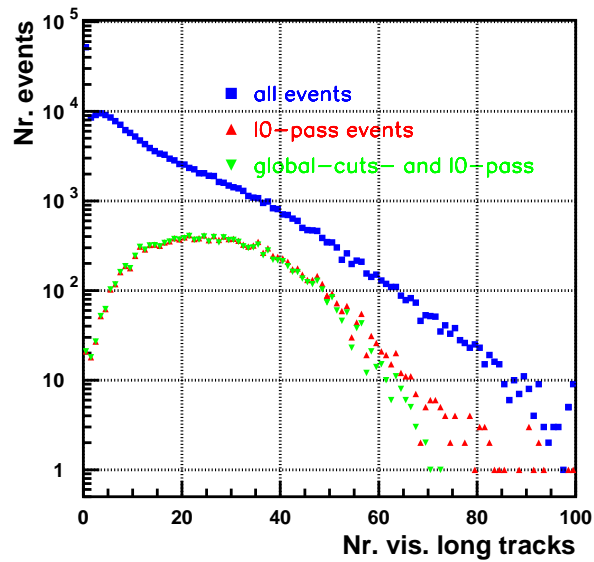


Figure 21: Distributions of the number of visible tracks for minimum-bias events and with the TDR L0DU.

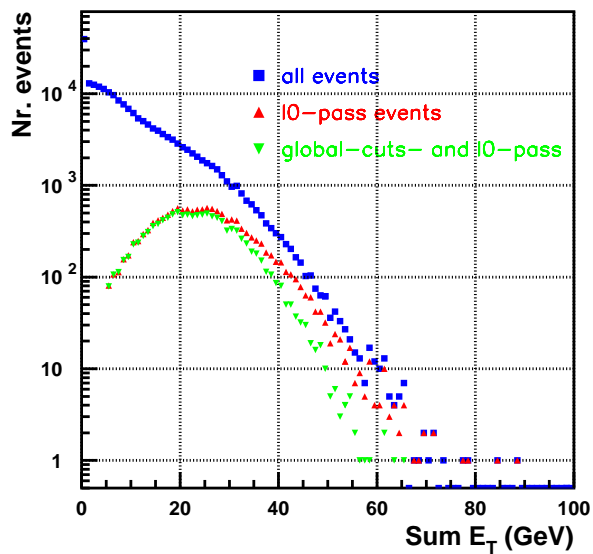


Figure 22: ΣE_T distributions for minimum-bias events and with scenario 4.

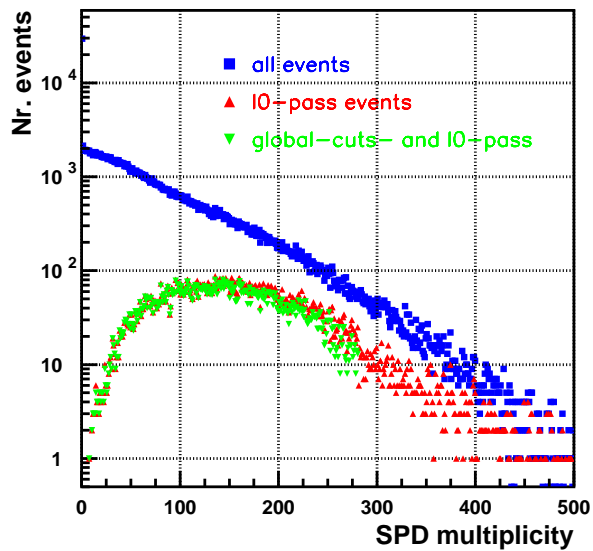


Figure 23: SPD multiplicity distributions for minimum-bias events and with scenario 4.

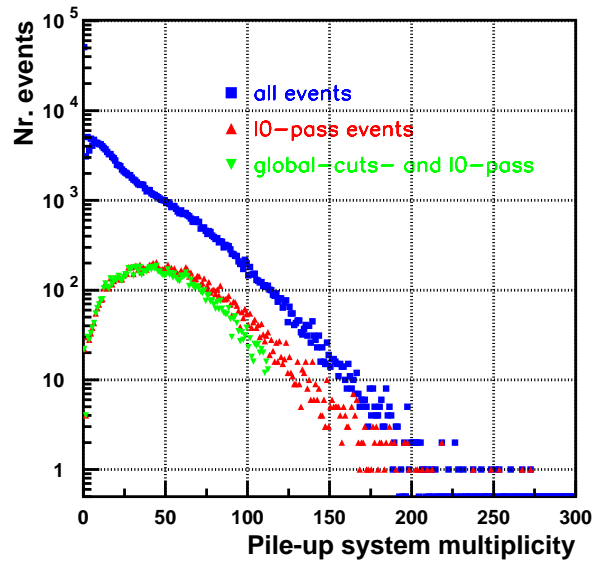


Figure 24: Pile-up system multiplicity distributions for minimum-bias events and with scenario 4.

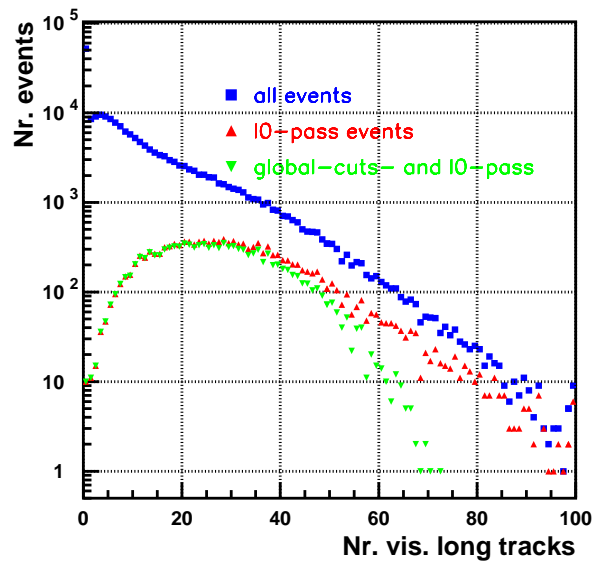


Figure 25: Distributions of the number of visible tracks for minimum-bias events and with scenario 4.

8 Implications for L1 and the HLT

In introducing in L0 extra ways to trigger on events that have been vetoed by our global event selection one should keep in mind the implications that such potentially complicated events (e.g. large multiplicities) can have on the processing in the higher levels of the trigger system – Level-1 (L1) and the High Level Trigger (HLT).

In figures 18-21 and 22-25 we present the distributions for the ΣE_T , the SPD multiplicity, the Pile-up System multiplicity and the number of visible tracks ¹, using the TDR L0DU and scenario 4, respectively. Distributions are shown for all minimum-bias events, for those that pass L0, and for those that pass L0 although they had been rejected by the global event selection. A comparison of the last 2 categories gives a clear indication of the nature of those extra events that make it to L1 thanks to the overriding sub-triggers. In both cases of the TDR L0DU and scenario 4 the bulk of those extra events is seen to have large track multiplicity (often more than 70 tracks) and also large SPD and Pile-up system multiplicities. The effect is more pronounced for scenario 4.

For completeness table 20 gives the percentage of minimum-bias and offline selected B-signal events that do not pass the global event selection but still make it to L1 because of an overriding sub-trigger. This percentage is seen to be lowest with the TDR L0DU, of the order of 25% for muon channels and 4–5% for (most of) all others. As expected the percentage for muon channels remains unchanged in all scenarios, since we kept the muon triggers bandwidth constant. For all scenarios, which, in comparison with the TDR, have (di-)electron overriding triggers, the percentages of "overridden" events for hadronic channels jump from 4–5% to 10–15%. And as with the muon channels also $\approx 25\%$ of the selected "e⁺e⁻" events are overridden. The situation is similar for minimum-bias events, with percentages 12–18% for scenarios 1-4, to be compared with a 5% with the TDR L0DU.

9 Conclusions and Final Remarks

In this note we have investigated the improvement in the performance of the first level trigger that can be obtained with the inclusion of a di-electron trigger similar to the present di-muon trigger. We also compared this modification with alternative solutions that do not require the need for the second highest- E_T electron at L0.

The inclusion of a di-electron trigger significantly improves the L0 performance for electromagnetic channels while keeping all other channels efficiencies basically unchanged (in fact small improvements are often achieved for the other channels) with respect to the

¹A track is considered "visible" if it has sufficient hits in the VELO and T1-3 to allow it to be reconstructible.

results presented in the Trigger TDR. But there are, unfortunately, drawbacks to the introduction of a di-electron trigger at L0: at the hardware level, the practical implementation needed to give access to the information on the second highest- E_T L0-electron candidate would require a modification in the selection crate. This fact motivated the study of simpler alternatives that make use of our present L0 hardware design.

We have proven that both these alternative electron triggers allow to improve the performance of L0 in the same way as the di-electron trigger – though the improvement for b -hadron $\rightarrow J/\psi + X \rightarrow (\mu^+ \mu^-) + X$ decays is about 10–20% worse.

We are brought to conclude that at the very least an "elegant solution" like a double-threshold electron trigger could and should be foreseen in the future. But if possible, a real estimation of the practical (mainly hardware-related) implications of the adaptation of a di-electron trigger would be desirable.

From a more general point of view it seems likely that double-threshold triggers will come to play an increasingly important role in the future developments of the L0DU algorithms. In particular, it may prove profitable to introduce double-thresholds to trigger – with a high cut – on tagging leptons rather than on the signal-B decay products.

Correlations between trigger levels are also an important factor to take into account in a global trigger optimization. The relevance of extra "global-vetoed" events (cf. previous paragraph) for offline analysis is ultimately dictated by our ability to use them successfully offline and to reconstruct them in the higher trigger levels. As the analyses evolve and improve one should always foresee the possibility of a system capable of triggering on these events.

Acknowledgements:

This Research has been supported by a Marie Curie Fellowship of the European Community Program "Improving Human Research Potential and the Socio-economic Knowledge Base" under contract number HPMF-CT-2002-01708.

I would like to thank Hans Dijkstra for numerous and very fruitful discussions and all feedback.

References

- [1] A. Papadelis, *Study of the use of dielectrons from $B \rightarrow J/\psi(e^+e^-)$ at L1*, LHCb Trigger Note LHCb 2003-096
- [2] The LHCb Collaboration, R. A. Nobrega *et al.*, *LHCb Trigger System Technical Design Report*, CERN/LHCC 2003-031, LHCb TDR 10, 2003
- [3] The LHCb Collaboration, R. A. Nobrega *et al.*, *LHCb Reoptimized Detector Design and Performance Technical Design Report*, CERN/LHCC 2003-030, LHCb TDR 9, 2003
- [4] H. Terrier, B. Pietrzyk, $B^0 \rightarrow J/\psi(ee)K_S^0$ selection, LHCb Note LHCb 2003-125
- [5] G. Pakhlova, I. Belyaev, *Radiative decays with LHCb*, LHCb Note LHCb 2003-090
- [6] S. Amato *et al.*, *The LHCb sensitivity to $\sin 2\beta$ from $B^0 \rightarrow J/\psi(\mu\mu)K_S$ asymmetry*, LHCb Note LHCb 2003-107
- [7] G. Raven, *Selection of $B_s \rightarrow J/\psi\phi$ and $B^+ \rightarrow J/\psi K^+$* , LHCb Note LHCb 2003-118
- [8] G. Balbi *et al.*, *Selection of $B_{(s)}^0 \rightarrow h^+h^-$ decays at LHCb*, LHCb Note LHCb 2003-123
- [9] A. Golutvin *et al.*, $B_s^0 \rightarrow D_s^\pm K^\mp$ and $B_s^0 \rightarrow D_s^- \pi^+$ event selection, LHCb Note LHCb 2003-127
- [10] F. Machefert *et al.*, $B^0 \rightarrow \pi^+ \pi^- \pi^0$ reconstruction with the re-optimized LHCb detector, LHCb Note LHCb 2003-077
- [11] E. Rodrigues, *Level-0 Trigger Bandwidth Division*, LHCb Trigger Note LHCb 2003-048
- [12] E. Rodrigues, *Comments on the Electromagnetic Triggers and the Hadronic Channels*, LHCb Trigger Note LHCb 2004-015, in preparation